SOFT ROBOTICS
Volume 00, Number 00, 2018

DOI: 10.1089/soro.2017.0097

SoRo
Soft Robotics

ORIGINAL ARTICLE

A Modular Soft Robotic Wrist for Underwater Manipulation

Shunichi Kurumaya,[1] Brennan T. Phillips,[2–4] Kaitlyn P. Becker,[2] Michelle H. Rosen,[2] David F. Gruber,[5] Kevin C. Galloway,[6] Koichi Suzumori,[1] and Robert J. Wood[2,3]

Abstract

This article presents the development of modular soft robotic wrist joint mechanisms for delicate and precise manipulation in the harsh deep-sea environment. The wrist consists of a rotary module and bending module, which can be combined with other actuators as part of a complete manipulator system. These mechanisms are part of a suite of soft robotic actuators being developed for deep-sea manipulation via submersibles and remotely operated vehicles, and are designed to be powered hydraulically with seawater. The wrist joint mechanisms can also be activated with pneumatic pressure for terrestrial-based applications, such as automated assembly and robotic locomotion. Here we report the development and characterization of a suite of rotary and bending modules by varying fiber number and silicone hardness. Performance of the complete soft robotic wrist is demonstrated in normal atmospheric conditions using both pneumatic and hydraulic pressures for actuation and under high ambient hydrostatic pressures equivalent to those found at least 2300 m deep in the ocean. This rugged modular wrist holds the potential to be utilized at full ocean depths (>10,000 m) and is a step forward in the development of jointed underwater soft robotic arms.

Keywords: soft robotic arm, fiber-reinforced actuator, underwater manipulation

Introduction

The development of soft actuators is a highly active research topic, with direct applications for human-friendly robots,[1] human-like robot,[2–5] human-assist robots,[6–10] and medical devices owing to their flexibility, compliance, and straightforward fabrication. Soft actuators can achieve complex motions with relatively simple control, offering an advantage over conventional mechatronic systems.[11–19] Soft actuators are also practical due to their compatibility with pneumatic and hydraulic pressure from various fluids and gases, and have a demonstrated utility as a tough and robust solution for use in harsh environments.[11] They also offer unique advantages over traditional deep-sea actuators, such as hydraulic cylinders and electrical linear actuators, which are better suited for heavy-duty tasks. For these reasons, our research group has been developing soft actuators for delicate and precise manipulation in the deep sea. Initial progress was made with the development of ''boa''-type fiber-reinforced actuators and ''bellows''-type grippers, which were used to successfully collect fragile biological specimens in the deep sea.[20] This article focuses on the design, construction, and characterization of wrist modules that are intended for use with the existing soft grippers and other soft actuators currently in development, as shown in Figure 1a, and is a step forward in the development of complete underwater soft robotic arms.

Fiber-reinforced soft actuators can realize various motions such as bending, twisting, expansion, extension, and contraction by varying the fiber arrangement.[21] When an elastic body expands, its body extends orthogonal to the direction of wound fibers, while motion is deflected depending on the fiber arrangement. The influence of fiber angle on the deformation of fiber-reinforced soft actuators has been investigated in previous work,[22–24] however, other design parameters such as rubber hardness, number of fibers, and rubber thickness require further characterization. While various types of fiber-reinforced soft

[1]Department of Mechanical Engineering, Tokyo Institute of Technology, Tokyo, Japan.
[2]School of Engineering and Applied Science, Harvard University, Cambridge, Massachusetts.
[3]Wyss Institute for Biologically Inspired Engineering, Harvard University, Cambridge, Massachusetts.
[4]Department of Ocean Engineering, University of Rhode Island, Narragansett, Rhode Island.
[5]Department of Natural Sciences, Baruch College, City University of New York, New York, New York.
[6]School of Engineering, Vanderbilt University, Nashville, Tennessee.

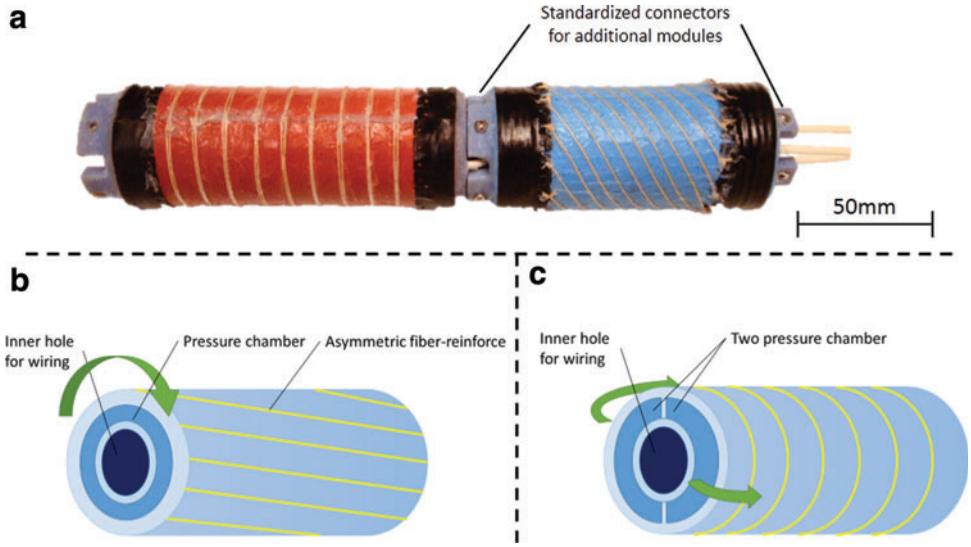

FIG. 1. **(a)** The soft wrist with bending (*left*) and rotary (*right*) modules attached in series. **(b)** Schematic overview of the rotary module having a pressurized chamber, asymmetric fibers, and inner hole for wiring. This module twists when the chamber is pressurized. **(c)** Schematic overview of the bending module having two pressurized chambers, circular fibers, and an inner hole for tubing and wiring. It bends in a direction opposite to the pressurized chamber. Color images available online at www.liebertpub.com/soro

actuators have been developed, fabrication processes vary widely and there are no existing standards for multiactuator integration. Furthermore, contemporary manipulator systems offer strength and multiple degrees of freedom, which are difficult to achieve using existing soft actuators. To overcome these challenges, we present a system based on fiber-reinforced soft actuators that are both scalable and modular (Fig. 1). Continuum robotic elements to marine applications made of rigid and partially soft materials have been developed in related works.[25–27] Modularity has a demonstrated utility in soft robotics to simplify control and increase system redundancy.[28] Our bending and rotary modules can be composed in series to form wrist, elbow, and shoulder joints.

In this article, we focus on two types of fiber-reinforced soft actuators that are scaled and arranged as a wrist mechanism. We report the development and characterization of these actuators by varying fiber number and silicone hardness with both pneumatic and hydraulic pressure. Water was chosen as a hydraulic fluid as it is a desirable medium for soft actuators.[29] Demonstrations of the soft robotic wrist operating with both pneumatic and hydraulic pressure are presented toward applications such as remote manipulation and robot-assisted assembly. In addition, a functionality test under high hydrostatic pressure was performed to assess the wrist's utility for deep-sea manipulation.

Design Overview

Several factors constrained the design of the soft wrist, which we developed with the goal of integrating into a complete manipulator system. One key aspect was modularity, which offers several advantages: specific components can be scaled independently, arranged in various sequences, and repaired and/or replaced with relative ease. Control of a full manipulator system is also simplified with discrete motions for each actuator. Using interchangeable gender-specific connectors, these actuators can be connected in series to achieve a desired working envelope. Internal passages for pressure lines and sensor integration were included to streamline the assembly. Both the connectors and the actuators themselves were designed with compactness in mind, to aid in approximating the behavior of a traditional multidegree-of-freedom joint.

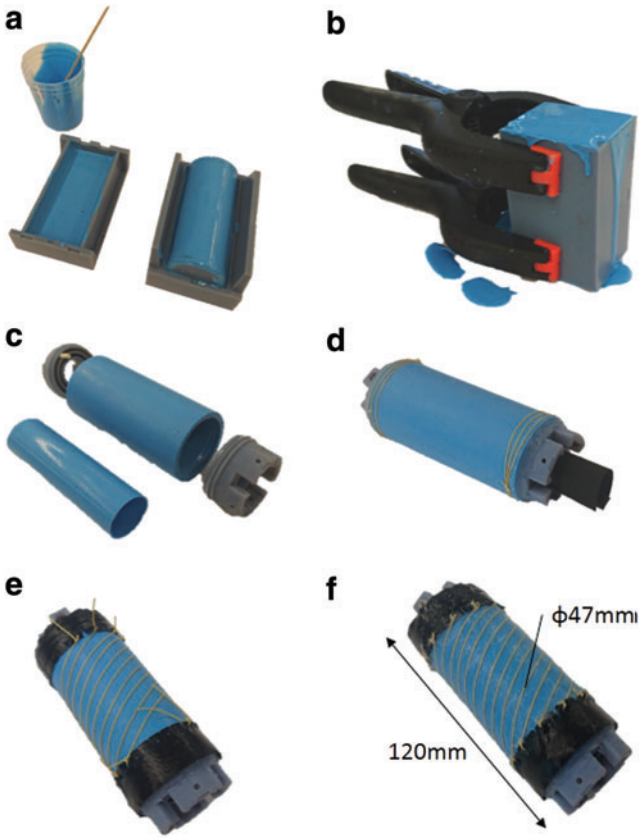

FIG. 2. Fabrication process of the rotary module. **(a)** Liquid silicone rubber (Smooth-Sil 950 by Smooth-On) is poured in both halves of 3D-printed molds. **(b)** The two mold halves are clamped together, and then, silicone rubber is formed into a cylindrical shape. **(c)** Silicone cylinders and three-dimensional (3D)-printed end connecters are combined by silicone adhesive (Sil-Poxy by Smooth-On). Both inner and outer cylinders are fabricated in the same manner. **(d)** Both ends are tightened by fibers and reinforced by nylon sheets. **(e)** Kevlar fibers are attached with a helical arrangement. **(f)** The completed actuator is coated with silicone adhesive. Color images available online at www.liebertpub.com/soro

Table 1. Specifications of the Rotary Module

Parameter	*Value*
Diameter of the outer cylinder	46 mm
Diameter of the inner cylinder	26 mm
Length	120 mm
Length of silicone part	70 mm
Hardness of the silicone	50 shore A
Fiber angle	30°
Number of outer fibers	12

The rotary module is a fiber-reinforced actuator with one degree of freedom consisting of an elastic cylinder surrounded by a helical arrangement of fibers (Fig. 1c). This design was optimized to achieve large angular motions with minimal axial displacement. The module has an interior passage for pressure and sensor lines, and a single sealed chamber for pressurization. The operation principle is the same as that of conventional fiber-reinforced actuators.[21,22] Expansion in the radial direction under applied internal pressure leads to twisting by extension in the vertical direction of the fibers. When pressure is released from the chamber, it returns to its original unactuated state.

The bending module is a fiber-reinforced actuator with a single degree of freedom, consisting of an elastic cylinder surrounded by a circular arrangement of fibers (Fig. 1b). This module has an inner hole for wiring and two symmetrical chambers for pressurization. When one chamber is pressurized, the module bends in a direction opposite the pressurized chamber, and when both chambers are pressurized the module extends in the axial direction. Typical operation requires one chamber to pressurize, while the opposite chamber is relieved of pressure.

Soft Module Development

Rotary module

The rotary module consists of seven basic parts: inner and outer cylinders, two end connectors, a pressure control tube, fibers, and nylon sheets. The fabrication process of the rotary module is described in detail in Figure 2. First, cylinder molds consisting of upper, inner, and outer parts are three-dimensional (3D) printed and liquid silicone rubber is poured into these molds (Fig. 2a). Next, the filled molds are combined and clamped together after removing any bubbles from the rubber (Fig. 2b). Once the silicone rubber has cured, the parts are removed. The two cured silicone cylinders and 3D-printed end connectors are combined using silicone adhesive (Fig. 2c). The supply tube is attached to one end connector. The actuator is then tightened by fibers and reinforced by nylon taffeta sheets (70 denier, heat sealable) outside and inside, respectively. Nylon sheets serve not only to reinforce against overpressurization but also as an anchor to affix fibers (Fig. 2d). Kevlar fibers are then attached in a helical arrangement to a pattern laser cut onto a nylon sheet (Fig. 2e). Finally, the entire actuator is coated in silicone glue to prevent slipping of the helical fibers (Fig. 2f).

Specifications of the rotary module are listed in Table 1. Fiber angle is determined from previous work[20] that reported an optimal twisting angle using fibers arranged at a 30° angle. The range of motion of a fiber-reinforced actuator under a specific pressure usually depends on the aspect ratio of wall thickness and diameter; the wall thickness of the rotary module was chosen to be similar to a flexible microactuator described in previous work.[22] The module twists in the direction of the fibers' offset angle, with some expansion and extension when pressurized (Fig. 3). The fabricated module twists 77° under an air pressure of 172 kPa and can achieve 90° rotation at 210 kPa. These pressures are similar to those used in soft gripping actuators developed for deep-sea sampling.[20]

Bending module

The bending module also consists of seven basic parts: two half-cylinder chambers, two end connectors, a pressure control tube, fibers, and nylon sheets. The fabrication process of the bending module is described in detail in Figure 4 and is similar to that of the rotary module. First, half-cylinder chamber molds consisting of upper, inner, and outer parts are 3D printed and liquid silicone rubber is poured into these molds (Fig. 4a). Next, these molds are combined and clamped together after removing bubbles (Fig. 4b). Once the silicone rubber has cured, the parts can be removed. Two half-cylinder chambers can be made in the same mold. A nylon sheet is put between the chambers and glued together with silicone adhesive to reinforce the inner sides of the chamber, and prevents extension in the center (Fig. 4c). 3D-printed end connectors are then attached with silicone adhesive and the pressure control tube is attached to an end connector (Fig. 4d). Both ends are tightened by fibers and reinforced by nylon sheets outside and inside, respectively (Fig. 4e). Kevlar fibers are then attached in a circular arrangement and the actuator is coated with silicone to prevent fibers from moving out of position (Fig. 4f).

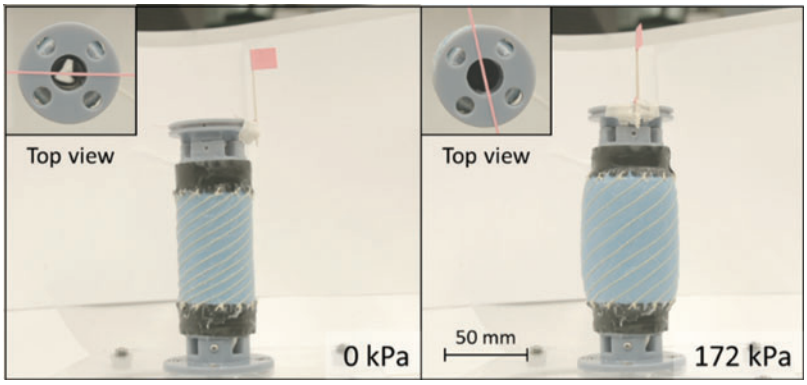

FIG. 3. Top and side view of the rotary actuator with 30° fiber angle. It twists 77° and extends 11 mm in the axial direction under an air pressure of 172 kPa. Color images available online at www.liebertpub.com/soro

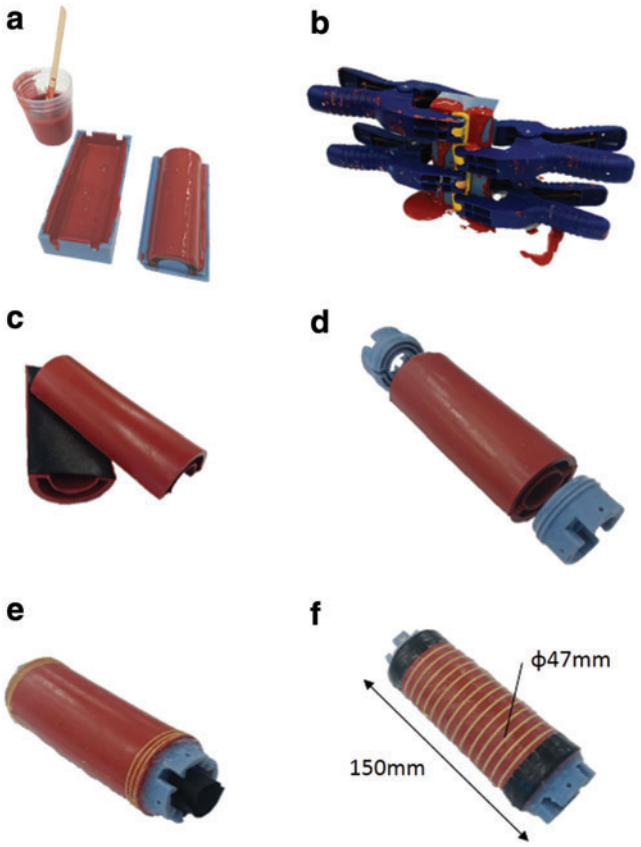

FIG. 4. Fabrication process of the bending module. **(a)** Liquid silicone rubber (M4601 by Wacker Chemical) is poured in both halves of 3D-printed molds. **(b)** The two mold halves are clamped together, and then, silicone rubber is formed into a half-cylindrical shape. **(c)** Nylon sheet is put between two half cylinders and these are assembled by silicone adhesive. **(d)** Fabricated silicone cylinders and 3D-printed end connecters are combined with silicone adhesive. **(e)** Both ends are tightened by fibers and reinforced by nylon sheets outside and inside, respectively. **(f)** Kevlar fibers are attached with a circular arrangement of fibers and the cylinder is coated with silicone. Color images available online at www.liebertpub.com/soro

Specifications of the bending module are shown in Table 2. Each design parameter was chosen to match that of the rotary module. The fiber angle is maximized at 0° fiber angle, since bending motion occurs via symmetric extension from a single chamber when pressurized (Fig. 5). Some asymmetry in the bending angles of each side can occur due to errors in fabrication.

TABLE 2. SPECIFICATIONS OF THE BENDING MODULE

Parameter	*Value*
Diameter of the outer cylinder	46 mm
Diameter of the inner cylinder	26 mm
Length	150 mm
Length of silicone part	100 mm
Hardness of the silicone	30 shore A
Fiber angle	0°
Number of outer fibers	14
Fiber interval	6.7 mm

Joint system

All modules have standardized gender-specific connectors (Fig. 6a). The joint is mechanically connected by #6–32 screws and nuts. Space in the female joint is reserved for tubing and wiring to run inside or outside the actuator (Fig. 6b). Thanks to the standardized joint system, modules are easily and quickly assembled and rearranged to achieve a desired workspace. Once modules connect to each other, all supply tubes and wires can run through the inner holes (Fig. 6c). Inner holes in the current design are capable of routing more than 20 3-mm-diameter tubes.

Characterization

Basic characteristics

To characterize the rotary and bending modules, four experiments under pneumatic pressure were conducted. First, the range of motion under varying pneumatic pressures was measured visually. Second, the torque of the rotary actuator and the applied force of the bending actuator were measured by using a materials characterization system (model: Instron 5544A, single column) as shown in Figure 7. Third, the compliance of each module was also measured using the same instrument. Finally, the speed of actuation was observed. The torque T and rotation angle φ of the rotary module are calculated using Equations (1) and (2), respectively, where the pulley's diameter D, tension F, and Instron displacement Δd are indicated in Figure 7a:

$$T = \frac{D}{2} \cdot F \tag{1}$$

$$\varphi = \frac{\Delta d}{D} \tag{2}$$

For the bending module, bending force F was measured and the bending angle θ was calculated using Equation (3), where initial module length L and Instron displacement Δd are indicated in Figure 9b:

$$\theta = \tan^{-1} \frac{\Delta d}{L} \tag{3}$$

The characterization results of the rotary module are shown in Figure 8. The maximum rotary angle is measured to be 90°, the maximum torque is 0.43 N·m, and the actuation time reaching 0.25 N·m at 103 kPa is 5 s. This results in a primary delay time constant of $\sim$3 (defined as the time required to achieve 63.2% of maximum torque). The characterization results of the bending module are shown in Figure 9. The maximum bend angle is 122°, maximum force is 15.6 N, and actuation time reaching 16 N at 138 kPa is 6 s, resulting in a primary delay time constant of $\sim$2. Both modules display hysteresis due to the material properties of silicone rubber.

Characteristics by varying design parameters

In addition to their geometrical design, fiber-reinforced actuators have various design parameters such as fiber angle,

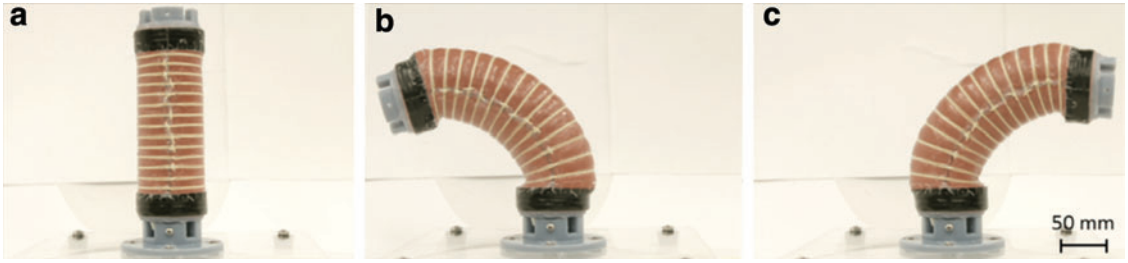

FIG. 5. Side view of the bending actuator with 0° fiber angle **(a)**. It bends 115° to the *left* **(b)** and 100° to the *right* **(c)** under an air pressure of 172 kPa. Color images available online at www.liebertpub.com/soro

number of fibers, and material elasticity that can be tuned to achieve the desired workspace. Focusing on the number of fibers and the hardness of silicone rubber, comparative tests were conducted to determine their effect on the rotary and bending actuators using both pneumatic and hydraulic pressure.

To determine the characteristics of the rotary module and bending module, a compliance experiment was conducted using the Instron materials characterization machine (as described in section 4.1). Rotary and bending modules with varying number of fibers and hardness of silicone rubber, as shown in Figure 10, were fabricated for these experiments. The specifications of the rotary and bending modules used in the compliance experiments are listed in Tables 3 and 4. The number of fibers can be also represented as a fiber interval, so the bending modules are described in terms of fiber interval. The relationship between torque and rotary angle or bending force and angle (i.e., compliance) was measured with the Instron machine moving from the actuated state at a particular pressure toward a length with no torque or bending force.

First, the compliance characteristics of the rotary module with varying number of fibers are shown in Figure 11 and with varying silicone rubber hardness in Figure 12. Comparison of the experimental values for torque and rotary angle is presented in Table 5. From these results, the following conclusions can be made.

(1) Rotary modules with hydraulic pressure show 3–11% higher torque than those with pneumatic pressure.
(2) Rotary modules with pneumatic pressure exhibit ~75–100% increased rotary angle than those with hydraulic pressure.
(3) The hardness of silicone rubber increases the maximum torque and rotary angle.
(4) The number of fibers increases the maximum torque and rotary angle.

Rotary modules with hydraulic pressure show increased torque and decreased rotary angle than those with pneumatic pressure because air is more compressible than water. The hardness of silicone dramatically influences compliance properties, making it an important design parameter. Harder silicone (50 shore A) is preferable, but if the module is operated at lower pressures, a softer silicone (30 shore A) is suitable. The number of fibers also influences compliance properties and performance increases in accordance with the fiber number. Furthermore, rotary modules can unevenly expand when there are too few fibers to constrain it. Although the number of fibers that can be attached to the module is limited, a dense fiber arrangement increases performance and durability.

The compliance characteristics of the bending module with varying number of fibers and silicone hardness are shown in

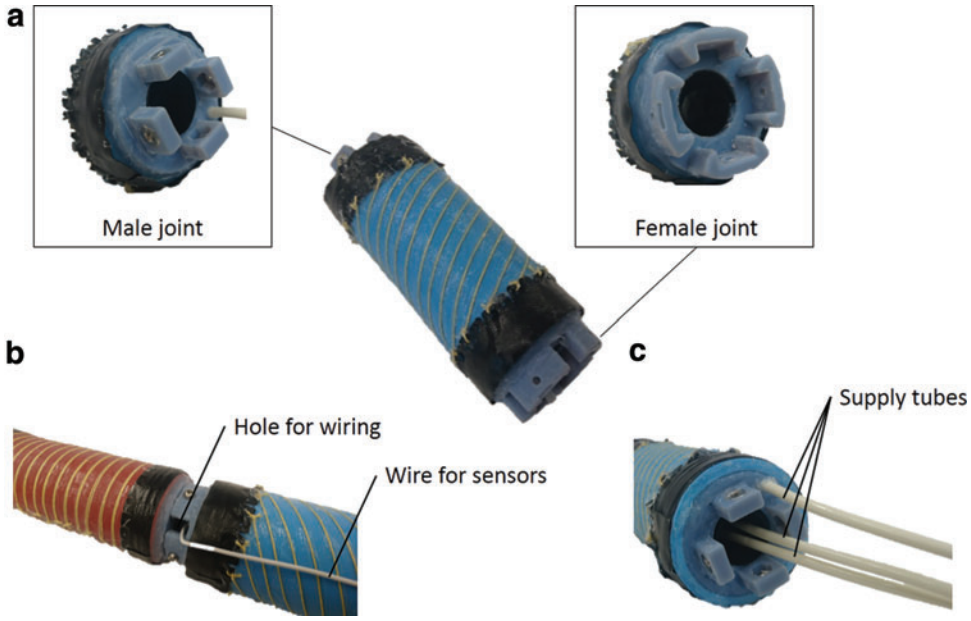

FIG. 6. Images of the joint system. **(a)** Male joint and female joint connected to each other by screws and nuts. **(b)** Side holes for sensor wiring. **(c)** Supply tubes can pass through the inner hole. Color images available online at www.liebertpub.com/soro

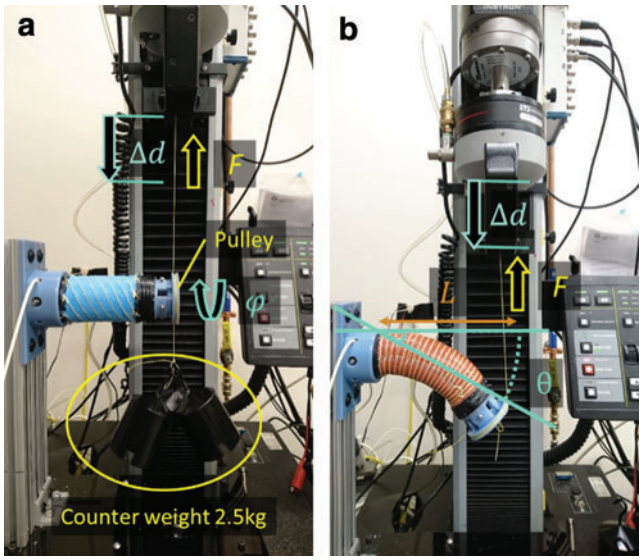

FIG. 7. Experimental setup for actuator characterization. **(a)** Rotary module with a counterweight of 2.5 kg to prevent bending. Torque was calculated by measuring force F using a 50-mm-diameter pulley, and rotary angle φ was visually observed. **(b)** Bending module. Bending force is observed as tension F by Instron, and bending angle is calculated by the actuator's displacement. The *circle* indicates position of the counter weight and *arrowheads* show the direction displacement and force. Color images available online at www.liebertpub.com/soro

Figures 13 and 14. A comparison of the experimental values for torque and rotary angle is presented in Table 6. From these results, the following conclusions can be made.

(1) Bending modules using hydraulic pressure exhibit linear compliance properties.
(2) Increasing silicone rubber hardness decreases the maximum bending force by 13–18% and reduces the bending angle by ∼50%.
(3) Among the fiber intervals tested, the bending force and bending angle are optimized with an interval of 6.7 mm.

As shown with the rotary module, bending modules with hydraulic pressure show linear compliance properties due to fluid compressibility. Similarly, the hardness of silicone dramatically influences compliance properties. Silicone rubber of 30 shore A hardness is preferable to that of 50 shore A due to material resistance to deformation. The number of fibers also influences compliance properties; however, bending force is not increased in accordance with the fiber number. In this experiment, we find that performance appears to be optimized with a fiber interval of ∼6.7 mm, which likely corresponds to a ratio related to the geometry of the actuator. If the fiber interval is too small, the minimized surface area of rubber limits expansion, and thus, extension area in the axial direction is decreased. If fiber interval is too large, expansion in the lateral direction is also increased and this limits the amount of force applied to bending, and thus, the extension area in the axial direction becomes small. A more exhaustive modeling and experimental effort are required to define a truly optimal relationship between fiber interval and actuator geometry.

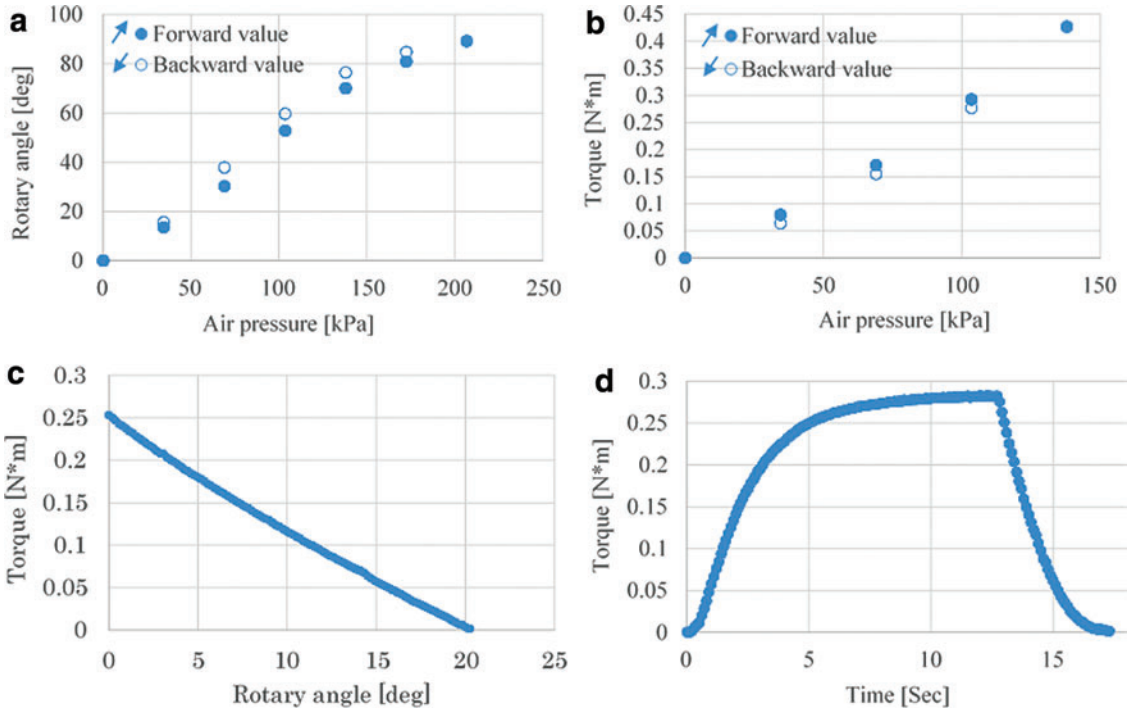

FIG. 8. Characterization of the rotary module. **(a)** Rotary angle under applied air pressure, where the maximum rotary angle is 90° at an air pressure of 207 kPa. **(b)** Torque under applied each pressure, where the maximum torque is 0.43 N·m at an air pressure of 138 kPa. **(c)** Compliance characteristics at an air pressure of 103 kPa. **(d)** The speed of actuation at an air pressure of 138 kPa, where the actuation time reaching 0.25 N·m is 5 s. Color images available online at www.liebertpub.com/soro

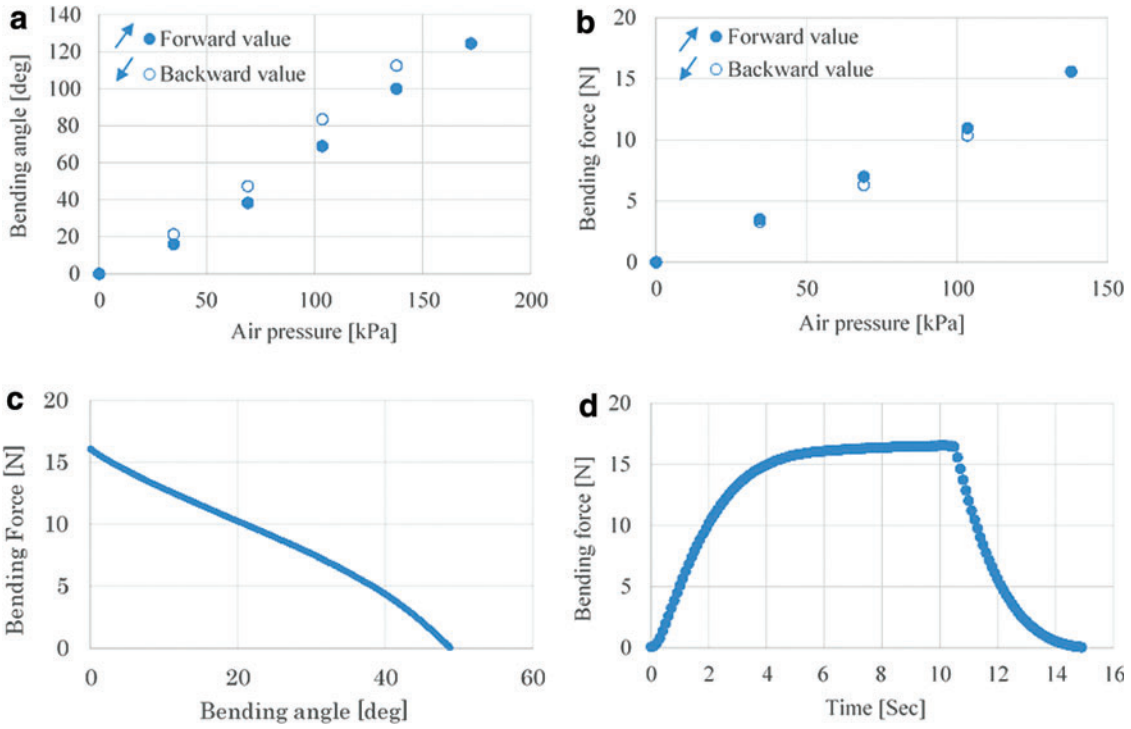

FIG. 9. Characterization of the bending module. **(a)** Bending angle under applied each pressure, where the maximum range of motion is 122° at an air pressure of 172 kPa. **(b)** Bending force under applied each pressure, where the maximum force is 15.6 N at an air pressure of 138 kPa. **(c)** Compliance characteristics at an air pressure of 138 kPa. **(d)** The speed of actuation at an air pressure of 138 kPa, where the actuation time reaching 16 N is 6 s. Color images available online at www.liebertpub.com/soro

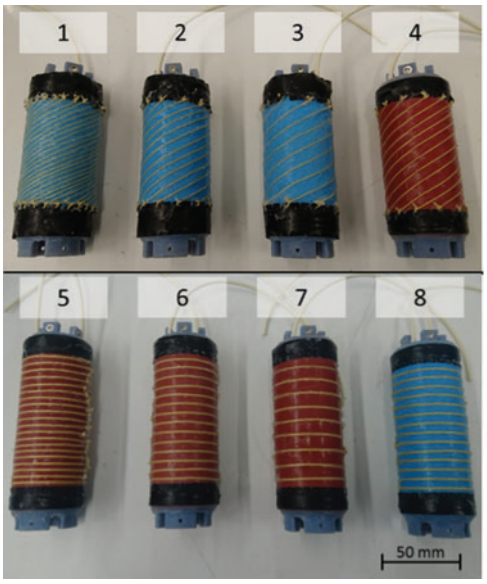

FIG. 10. Rotary modules (Nos. 1–4) shown with various number of fibers and hardness of silicone rubber. Specific properties are listed in Table 3. Bending modules (Nos. 5–8) shown with various number of fibers (fiber interval) and hardness of silicone rubber. Specific properties are listed in Table 4. Color images available online at www.liebertpub.com/soro

Soft Wrist Demonstration

A soft robotic wrist with two degrees of freedom is created by combining rotary and bending modules, and additional actuators can be attached to either end for various manipulation tasks. The working range of motion at the tip of the wrist was obtained using a Vicon motion capture system, and encompasses a hemisphere of 140-mm radius bounded by the

TABLE 3. SPECIFICATIONS OF THE ROTARY MODULE USED FOR COMPARISON

No.	*Length of silicone part (mm)*	*No. of fibers*	*Hardness of silicone rubber (shore A)*
1	70	24	50
2	70	12	50
3	70	8	50
4	70	12	30

TABLE 4. SPECIFICATIONS OF THE BENDING MODULE USED FOR COMPARISON

No.	*Length of silicone part (mm)*	*No. of fibers*	*Fiber interval (mm)*	*Hardness of silicone rubber (shore A)*
5	100	19	5	30
6	100	14	6.7	30
7	100	9	10	30
8	100	14	6.7	50

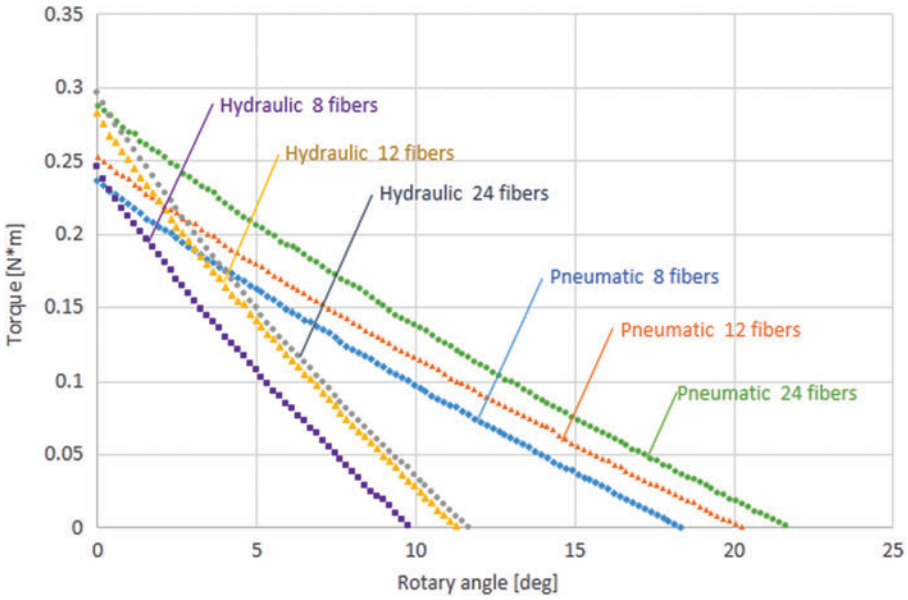

FIG. 11. Compliance characteristics of rotary modules by varying the number of fibers under a maintained pressure of 103 kPa. Color images available online at www.liebertpub.com/soro

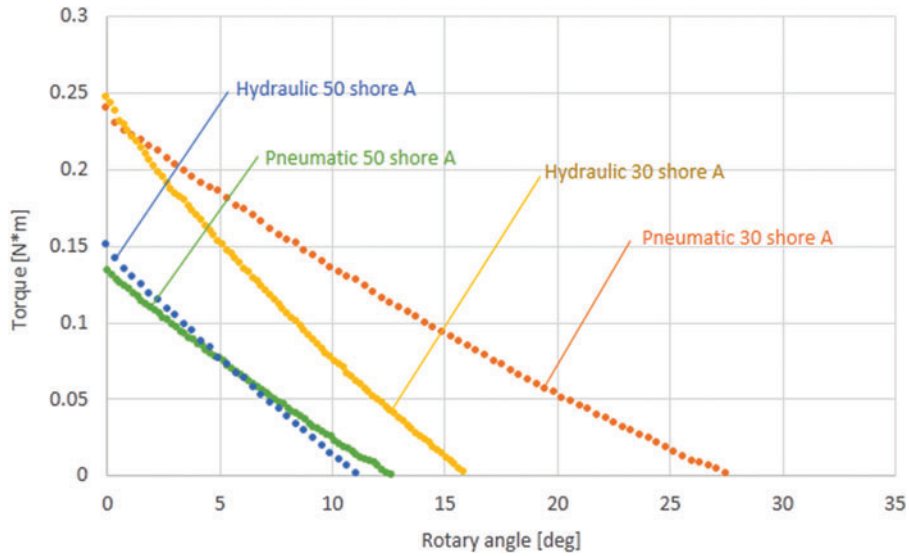

FIG. 12. Compliance characteristics of rotary module by varying the hardness of silicone rubber under a maintained pressure of 63 kPa. Color images available online at www.liebertpub.com/soro

rotary actuator's twisting range of ~90° (Fig. 15). This workspace is similar in scale to the existing soft manipulators developed recently.[30,31] We envision increasing the workspace of the soft wrist by using additional modules.

A functionality test was conducted at a high-pressure test facility (Woods Hole Oceanographic Institution) to demonstrate the wrist's performance under high hydrostatic pressures (Fig. 16; see also Supplementary Video S1; Supplementary Data are available online at www.liebertpub.com/soro). Actuation was successfully achieved using similar hydraulic pressures presented in section 4, which were elevated above the ambient pressure of 24 MPa (equivalent to 2300 m seawater depth) with no apparent limitation in the actuator's range of motion. Following the test, the actuators showed no signs of damage and were completely functional at normal atmospheric pressure.

Table 5. Comparison of Experimental Values for Torque and Rotary Angle at 103 kPa Pneumatic or Hydraulic Pressure

	No. 1	*No. 2*	*No. 3*	*No. 4*[a]
Maximum torque with pneumatic pressure	0.288 N·m	0.253 N·m	0.237 N·m	0.241 N·m
Maximum torque with hydraulic pressure	0.297 N·m	0.283 N·m	0.246 N·m	0.247 N·m
Maximum rotary angle with pneumatic pressure	21.8°	20.4°	18.5°	27.9°
Maximum rotary angle with hydraulic pressure	11.8°	11.5°	9.9°	16.0°

[a]Maximum torque and rotary angle of No. 4 were pressurized at 63 kPa.

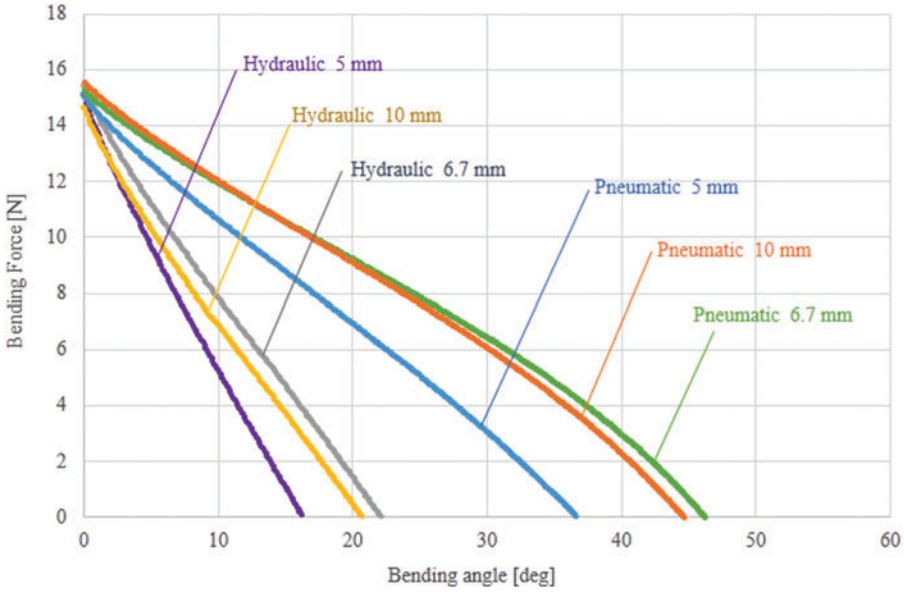

FIG. 13. Compliance characteristics of bending modules by varying the fiber interval under a maintained pressure of 138 kPa. This measurement was performed by releasing tension. Color images available online at www.liebertpub.com/soro

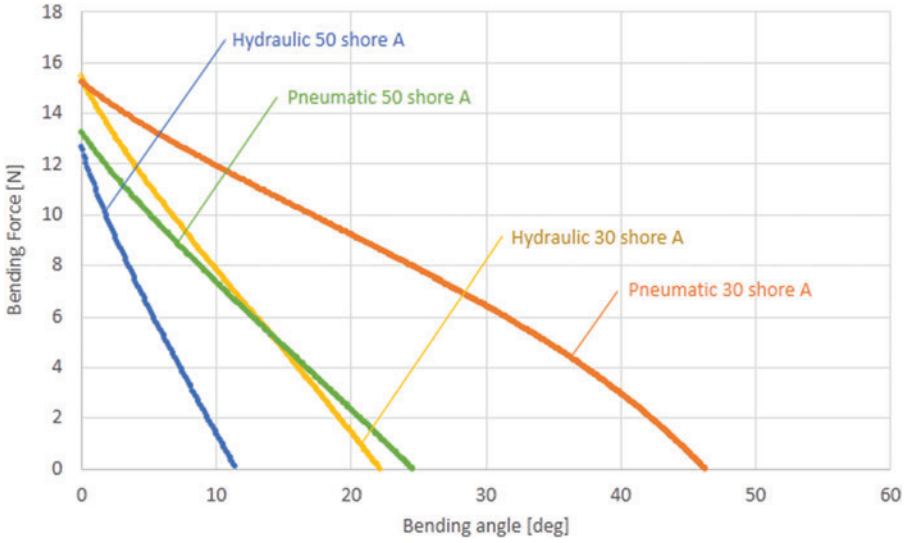

FIG. 14. Compliance characteristics of bending modules by varying the hardness of silicone rubber under a maintained pressure of 138 kPa. This measurement was performed by releasing tension. Color images available online at www.liebertpub.com/soro

Conclusions and Future Work

We presented the design, fabrication, and characterization of a new class of modular fiber-reinforced actuators. Two different designs are demonstrated: a rotary actuator capable of up to 90° rotation with a maximum torque of 0.43 N·m, and a bending actuator that can curve ±120° in opposing directions and apply a force of 15.6 N. Actuation characteristics of these modules using both pneumatic and hydraulic pressure are presented, along with the impacts of varying material selection and fiber arrangement. The actuators are designed with a standardized joint mechanism, and their use as a complete wrist assembly is demonstrated under normal atmospheric pressure and high hydrostatic pressure.

Our rotary and bending modules are similar in scale to a human wrist, making them ideal candidates for a human-scale

Table 6. Comparison of Experimental Values for Bending Force and Bending Angle at 138 kPa Pneumatic or Hydraulic Pressure

	No. 5	*No. 6*	*No. 7*	*No. 8*
Maximum bending force with pneumatic pressure	15.0 N	15.3 N	15.6 N	13.3 N
Maximum bending force with hydraulic pressure	15.1 N	15.4 N	14.6 N	12.7 N
Maximum bending angle with pneumatic pressure	36.7°	46.3°	44.7°	24.6°
Maximum bending angle with hydraulic pressure	16.3°	22.2°	20.8°	11.5°

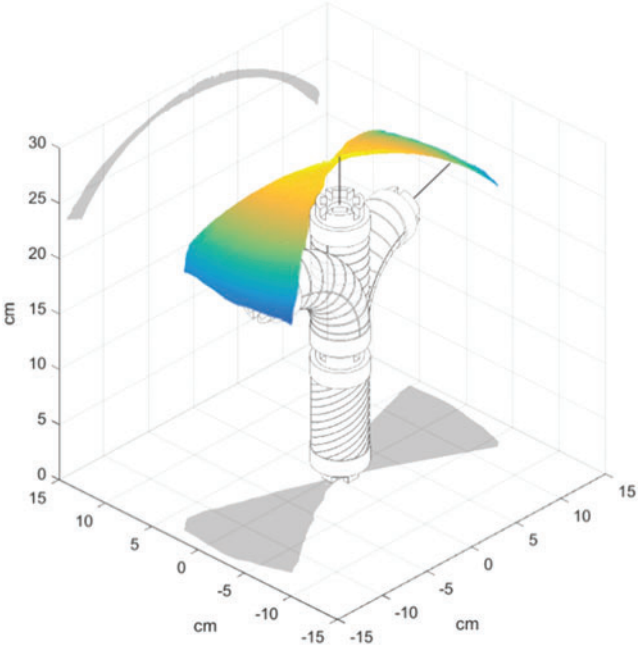

FIG. 15. The workspace of the soft wrist; model is shown to scale. Color images available online at www.liebertpub.com/soro

manipulator system. This work is part of a series of steps toward controllable soft robotic arms and grippers that are designed for robust, remote manipulation. Using hydraulic pressure, they are particularly suited for work in the marine environment and have direct applications for sampling of delicate biological specimens. We also envision other practical applications, such as robot-assisted assembly, logistics, agriculture, and surgical manipulation.

In the near future, we anticipate field testing these actuators as part of a complete manipulator system in the deep sea. The design of the modules would benefit from further refinement, with a focus on increasing their ability to handle higher pressures to achieve a higher range of motion and force application. The actuators would also benefit from having proprioceptive sensors toward a haptic control interface and autonomous manipulation motions.

FIG. 16. Performance test using hydraulic pressure in a high-pressure test facility. Ambient pressure surrounding the actuators is 24 MPa, equivalent to 2300 m seawater depth. A video of actuation is provided in Supplementary Video S1. Color images available online at www.liebertpub.com/soro

Acknowledgments

This study was funded by NSF Instrument Development for Biological Research Award #s 1556164 to R. Wood and K. Galloway and #1556123 to D. Gruber. Any opinions, findings, and conclusions or recommendations expressed in this material are those of the authors and do not necessarily reflect the views of the National Science Foundation. The authors express their sincere appreciation to James Weaver and Alex Meckes for their assistance in 3D printing and mold design.

Author Disclosure Statement

No competing financial interests exist.

References

1. Tsagarakis NG, Laffranchi M, Vanderborght B, Caldwell DG. A compact soft actuator unit for small scale human friendly robots. In: Proceedings of the 2009 IEEE International Conference on Robotics and Automation. Kobe International Conference Center, Kobe, Japan, May 12–17, 2009, pp. 4356–4362.
2. Kurumaya S, Suzumori K, Nabae H, Wakimoto S. Musculoskeletal lower-limb robot driven by multifilament muscles. ROBOMECH J 2016;3:18.
3. Niiyama R, Nagakubo A, Kuniyoshi Y. Mowgli: A bipedal jumping and landing robot with an artificial musculoskeletal system. In: Proceedings of the 2007 IEEE International Conference on Robotics and Automation. Roma, Italy, April 10–14, 2007, pp. 2546–2551.
4. Hosoda K, Takuma T, Nakamoto A, Hayashi S. Biped robot design powered by antagonistic pneumatic actuators for multi-modal locomotion. Rob Auton Syst 2008;56:46–53.
5. Sanan S, Lynn PS, Griffith ST. Pneumatic torsional actuators for inflatable robots. J Mech Robot 2014;6:031003.
6. Kawamura S, Hayakawa Y, Tamai M, Shimizu T. A design of motion-support robots for human arms using hexahedron rubber actuators. In: Proceedings of the 1997 IEEE/RSJ International Conference on Intelligent Robots and Systems, Grenoble, France, September 11, 1997, pp. 1520–1526.
7. Sanan S, Ornstein MH, Atkeson CG. Physical human interaction for an inflatable manipulator. In: Proceedings of the 33rd Annual International Conference of the IEEE EMBS, Boston, MA, August 30–September 3, 2011, pp. 7401–7404.
8. Okui M, Iikawa S, Yamada Y, Nakamura T. Fundamental characteristic of novel actuation system with variable viscoelastic joints and magneto-rheological clutches for human assistance. J Intell Mater Syst Struct 2017;29:82–90.
9. Ohno A, Nabae H, Suzumori K. Static analysis of powered low-back orthosis driven by thin pneumatic artificial muscles considering body surface deformation. In: Proceedings of the 2015 IEEE/SICE International Symposium on System Integration, Nagoya, Japan, December 11–13, 2015, pp. 39–44.
10. Hiroshi K, Ishida Y, Suzuki H. Realization of all motion for the upper limb by a muscle suit. In: Proceedings of the IEEE International Workshop on Robot and Human Interactive Communication, ROMAN. Okayama, Japan, September 20–22, 2004, pp. 631–636.
11. Roche ET, Wohlfarth R, Overvelde JTB, Vasilyev NV, Pigula FA, Mooney DJ, *et al.* A bioinspired soft actuated material. Adv Mater 2014;26:1200–1206.

12. Polygerinos P, Wang Z, Galloway KC, Wood RJ, Walsh CJ. Soft robotic glove for combined assistance and at-home rehabilitation. Rob Auton Syst 2015;73:135–143.
13. Ilievski F, Mazzeo AD, Shepherd RF, Chen X, Whitesides GM. Soft robotics for chemists. Angew Chem Int Ed 2011; 50:1890–1895.
14. Martinez RV, Fish CR, Chen X, Whitesides GM. Elastomeric origami: programmable paper-elastomer composites as pneumatic actuators. Adv Funct Mater 2012; 22:1376–1384.
15. Martinez RV, Branch JL, Fish CR, Jin L, Shepherd RF, Nunes RMD, Suo Z, Whitesides GM. Robotic tentacles with three-dimensional mobility based on flexible elastomers. Adv Mater 2013;25:205–212.
16. Wakimoto S, Suzumori K, Ogura K. Miniature pneumatic curling rubber actuator generating bidirectional motion with one air-supply tube. Adv Robot 2011;25:1311–1330.
17. Shepherd RF, Stokes AA, Nunes RMD, Whitesides GM. Soft machines that are resistant to puncture and that self seal. Adv Mater 2013;25:6709–6713.
18. Majidi C. Soft robotics: a perspective—current trends and prospects for the future. Soft Robot 2013;1:5–11.
19. Trivedi D, Rahn CD, Kier WM, Walker ID. Soft robotics: biological inspiration, state of the art, and future research. Appl Bionics Biomech 2008;5:99–117.
20. Galloway KC, Becker KP, Phillips BT, Kirby J, Licht S, Tchernov D, *et al.* Soft robotic grippers for biological sampling on deep reefs. Soft Robot 2016;3:23–33.
21. Connolly F, Polygerinos P, Walsh CJ, Bertoldi K. Mechanical programming of soft actuators by varying fiber angle. Soft Robot 2015;2:26–32.
22. Suzumori K, Iikura S, Tanaka H. Development of flexible microactuator and its applications to robotic mechanisms. IEEE Int Conf Robot Autom 1991:1622–1627.
23. Galloway KC, Polygerinos P, Walsh CJ, Wood RJ. Mechanically programmable bend radius for fiber-reinforced soft actuators. In: Proceedings of the 1991 IEEE International Conference on Robotics and Automation, Sacramento, CA, April 1991, pp. 1–6.
24. Bishop-Moser J, Krishnan G, Kim C, Kota S. Design of soft robotic actuators using fluid-filled fiber-reinforced elastomeric enclosures in parallel combinations. In: Proceedings of the 16th International Conference on Advanced Robotics, Montevideo, Uruguay, November 25–29, 2014, pp. 4264–4269.
25. Onal CD, Rus D. A modular approach to soft robots. In: Proceedings of the 2012 IEEE/RSJ International Conference on Intelligent Robots and Systems, Vilamoura, Portugal, October 7–12, 2012, pp. 1038–1045.
26. Lane DM, Davies JBC, Robinson G, O'Brien DJ, Sneddon J, Seaton E, *et al.* The AMADEUS dextrous subsea hand: design, modeling, and sensor processing. IEEE J Oceanic Eng 1999;24.1:96–111.
27. Scott GP, Henshaw CG, Walker ID, Willimon B. Autonomous robotic refueling of an unmanned surface vessel in Varying Sea States. IEEE/RSJ Int Conf Robot Intell Syst 2015:1664–1671.
28. Sfakiotakis M, Kazakidi A, Chatzidaki A, Evdaimon T, Tsakiris D. Multi-arm robotic swimming with octopus-inspired compliant web. In: Proceedings of the 2015 IEEE/RSJ International Conference on Intelligent Robots and Systems, Congress Center Hamburg, Hamburg, Germany, September 28–October 2, 2015, pp. 302–308.
29. Focchi M, Guglielmino E, Semini C, Parmiggiani A, Tsagarakis N, Vanderborght B, *et al.* Water/air performance analysis of a fluidic muscle. In: Proceedings of the 2014 IEEE/RSJ International Conference on Intelligent Robots and Systems, Chicago, IL, September 14–18, 2014, pp. 2194–2199.
30. Katzschmann RK, Marchese AD, Rus D. Autonomous object manipulation using a soft planar grasping manipulator. Soft Robot 2015;2:155–164.
31. Ranzani T, Gerboni G, Cianchetti M, Menciassi A. A bioinspired soft manipulator for minimally invasive surgery. Bioinspir Biomim 2015;10:035008.

Address correspondence to:
Shunichi Kurumaya
Department of Mechanical Engineering
Tokyo Institute of Technology
Tokyo 152-8552
Japan

E-mail: kurumaya.s.aa@m.titech.ac.jp